The Pennsylvania State University

Electrical Engineering Department

University Park, Pennsylvania 16802

MAPPING OF ELECTRICAL POTENTIAL DISTRIBUTIONS WITH CHARGED PARTICLE BEAMS

November 1977-February 1982
Final Report

National Aeronautics and Space Administration

Grant NSG-3166

James W. Robinson

February 1982

ABSTRACT

Two major activities comprise the work summarized in this report. The first of these is a study of methods for measuring electrostatic potentials on and near dielectric surfaces charged to several kilovolts. The other is the measurement of secondary emission from those charged dielectrics. Methods of potential measurement are measuring induced charge from which potential is calculated, measuring trajectory endpoints of either high or low energy particles traversing the region near the surface, observing trajectory impact on the surface, and creating ions at points of interest near the surface. Some of the methods require computer simulations and iterative calculation if potential maps are to be generated. Several approaches are described and compared. A method using a half-cylinder as a test chamber and low-energy probing beams is adapted for the measurement of secondary emission. The critical energy for a secondary emission coefficient of unity increases with increasing normal electric field and with age. The dependence upon angle of incidence is that predicted theoretically, $\cos^{-1}$ of the angle. However near the edges of the specimen where potential gradients are large and the electric field is tangential to the surface, the secondary emission coefficient tends toward unity for a wide variety of conditions.

CONTENTS

LIST OF FIGURES

ACKNOWLEDGEMENTS

The work reported here represents the efforts of several graduate students who not only spent many hours fabricating and measuring but who provided many insights and interpretations without which the work would not have been possible. Also many undergraduates contributed to the work at various times. These contributions are gratefully acknowledged. All of us at Penn State express our thanks to the group at NASA-Lewis under the direction of N. John Stevens which has provided the financial support and the encouragement to do this work.

1. REVIEW OF PROGRAM

1.1 Historical Perspective

The work reported under this grant has been part of a much larger joint program of NASA and USAF[1] initiated in the mid 1970's for the study of spacecraft charging phenomena. The need for such a program was apparent from cases of malfunction or complete failure which had been reported and from studies[2] which showed that constituents of substorm plasmas could charge spacecraft to high potentials. The work conducted under this grant is classified mainly as materials characterization, one area of emphasis in the joint program. However the measurement of secondary electron emission, this grant's activity related to characterization, required the development and use of techniques for measuring and simulating electric fields near the specimen. Several methods for doing these things were developed and tested. Furthermore it is noted that closely related work was performed earlier under NASA grant NSG-3097. The reports and papers generated from this and the previous grant are listed in the Appendix of this report.

1.2 Surface Charge Distributions

The cause of observed phenomena can be traced to the charging of dielectric surfaces located in a charged-particle environment.

Although both metals and dielectrics accumulate charges, the metals, which readily distribute the charges, have surface potentials that are controllable. The surface potentials of dielectrics, on the other hard, are influenced by several complex phenomena which have been the focus of numerous investigations. One of the first problems was that of measuring the potential distribution on a specimen which had been exposed to a charging environment. Such measurements then provided data from which electric fields and charge distributions could be calculated. Without such data other studies would not have been possible.

Though some experimenters have charged specimens with a spectrum of electron energies,[3] [4] the majority of investigations have been for normally incident, monoenergetic electrons. When thin, metal-backed dielectric films are charged with normally-incident, monoenergetic electrons of several kilovolts, then the following observations are made:[5]

1) The region away from the edges of the specimen charges to a potential less than that of the electrons by the amount of the critical energy, that energy for which the secondary emission coefficient is unity.

2) A potential gradient exists near a dielectric-metal interface, typically extending a few millimeters from the interface.

3) The surface charge pattern may be suddenly modified by a discharge tangential to the surface between the dielectric surface and the metal. The probability of discharge depends strongly on the design of the

interface.

When one has measured surface potential by any of several different methods, he can then calculate the charge distribution on the surface of the dielectric and also the electric fields in the region near the dielectric surface. Though such a calculation does not distinguish between the charges residing at different depths in the dielectric, it still yields a correct field pattern outside the surface. For the work conducted under this grant, the charges themselves have been of little interest but the fields have been used extensively for calculating particle trajectories.

1.3 Dynamics of Charging and Flashovers

Necessary for the work with secondary emission is the establishment of a stable, reproducible potential distribution on the surface of the specimen, a distribution which decays very slowly when the electron source is turned off. The material FEP-Teflon has been used almost exclusively because it holds a charge well and its characteristics have been found to be stable. When this material is exposed to a stream of electrons, it accumulates charge in different amounts on different portions of its surface until the secondary emission coefficient becomes unity at all points which the beam strikes. Then when the beam intensity is reduced to zero, the specimen remains in that charged state. It is important to note that even though the electron stream is normal to the surface, the incoming electrons are slowed and deflected by the accumulated surface charge so that, especially

near the edges of the specimen, the electrons strike the specimen at oblique angles.

The occurrence of a discharge would have spoiled the charge distribution which the electron source had established. Thus the dielectric-metal interfaces were designed to minimize the probability of discharge and the potentials were kept below levels which would cause a discharge. Experience has shown that the dielectric specimen should be exposed through an aperture in a thin, metal foil placed directly on the surface of the specimen.

Often the charge must be removed from the surface of the specimen. This is easily done by exposing the specimen to electrons of an energy which causes the secondary emission coefficient to be greater that unity. First the electron source is operated at its normal voltage and then, while the source continues to emit, the voltage is slowly reduced. Simultaneously the voltage on the specimen drops. One problem with this method is that the specimen does not return to its original charge state but that it develops a dipole layer of charges, negative charges deep below the surface and positive charges near the surface.[6] Ultraviolet radiation may be used instead of electrons.

When a specimen remains in vacuum for several days or weeks, it charges differently than at first. Certainly our results show the changes which occur, though the reasons are not clear. Perhaps the reasons depend upon the charge layer structure or perhaps upon the surface contamination. Results shown in reports

have generally come from specimens which were in vacuum at least for several days.

1.4 Noninvasive Measurements of Potential

Measuring surface potentials is one of the major emphases of this report. Instruments do exist which can measure surface potentials with probes placed near the surface, and such measurements can be quite satisfactory for many purposes. But one must ask, especially if a plasma is present, if the probe is perturbing what it is trying to measure. Also in many geometries, there is not physical space available for the probe. Because of the limitations of probes, noninvasive methods of measurement have been developed, tested, and some used as appropriate. The methods reviewed in this report are as follows:

1) Induced charge in the metal backing of the specimen.
2) Measurements in the vicinity of the surface with high-velocity non-impacting beams of charged particles.
3) Measurements in the vicinity of the surface with low-velocity non-impacting beams of charged particles.
4) Measurements with impacting beams.
5) Ion-release at the point of interest.
6) Combinations of the preceding.

Because the various methods of obtaining data are incomplete in themselves, an important feature of potential measurement is the processing of data. Various approaches are noted in this report and problems are identified. Of course the more extensive the data, the more extensive the map which may be made, but a

given set of data may contain ambiguities, different types for different situations. Some techniques are valid only for space-charge-free regions whereas others are more general, and some pertain only to regions with azimuthal symmetry.

1.5 Secondary Electron Emission

Secondary electron emission depends upon many factors, some of which are well known, and some whose effects have not been measured. This work investigates how electric fields influence secondary emission. The work is complicated by the fact that, when fields exist, they influence the trajectories of primary electrons so that the electrons do not strike the specimen at the place where they were aimed, or with the energy or angle which they had originally. One must know the fields in the vicinity of the specimen and calculate how the trajectories are modified so that a measurement of secondary emission can be associated with a particular point of impact, an energy, and an impact angle. Thus the work with potential measurement is essential for the measurements of the secondary emission coefficient.

Measurements have been made at different points on the specimens where the fields are quite different, some normal and some tangential, and measurements have been for different energies and angles. However a word of caution must be included. If the coefficient is measured at a certain location where field has a certain value, does the departure from the theoretical prediction represent the effect of the field, or is there possibly some other variable which has been overlooked? This

question will remain unanswered but the secondary coefficient can be identified with the field at each of the various points where it was measured

2. MEASUREMENTS WITH PROBING BEAMS

Numerous methods exist for measuring potential in the region near a dielectric surface, methods which do not require the insertion of any device, but which depend upon charged particles as the sensors. Also a measure of induced charge can provide information. This chapter classifies and evaluates several methods.

2.1 Possible Noninvasive Measurements of Potential

All methods described here depend upon the motion of charged particles except for those methods which depend upon induced charge. The method of induced charge requires measuring charge induced by the charged dielectric specimen in some nearby structure which is maintained at virtual ground. It is then inferred, with a knowledge of capacitance between the structure and the surface, what the surface potential must be. This method, described in the next section, depends upon the segmenting and the instrumenting of normally occurring ground structures which would be present even if no measurement were being made.

Aside from using induced charge, one may use several different methods for obtaining information about a region of space on or near the surface. The information associated with particle trajectories depends, in sometimes complicated ways, on the region through which the particles travel. Also if one is willing to disturb the charge on the dielectric surface, he can

get much useful information by letting the test particles strike the surface.

When magnetic fields exist, several methods may be employed, one being referenced here.[7] However these techniques are not applicable in the work described in this report.

When magnetic effects and induced charges are not included, the work with charged particles can be classified in the following ways:

1) High-energy particles which pass through the region.
2) Low-energy particles which impact or pass through the region.
3) Particles which are created in the region.

While each of these methods has advantages, sometimes a combination of methods can be much more effective than any one of them. These methods and combinations are discussed in more detail in the sections which follow.

2.2 Induced Charge

Measurements of this type[5] showed the characteristic edge gradients which appear near dielectric-metal interfaces. When the grounded metal film behind a thin specimen is segmented, and each segment is independently grounded either with a jumper wire or with the virtual ground of an electrometer, then the charges in each segment can be measured in turn and a profile constructed. Fig. 1 illustrates the procedure.

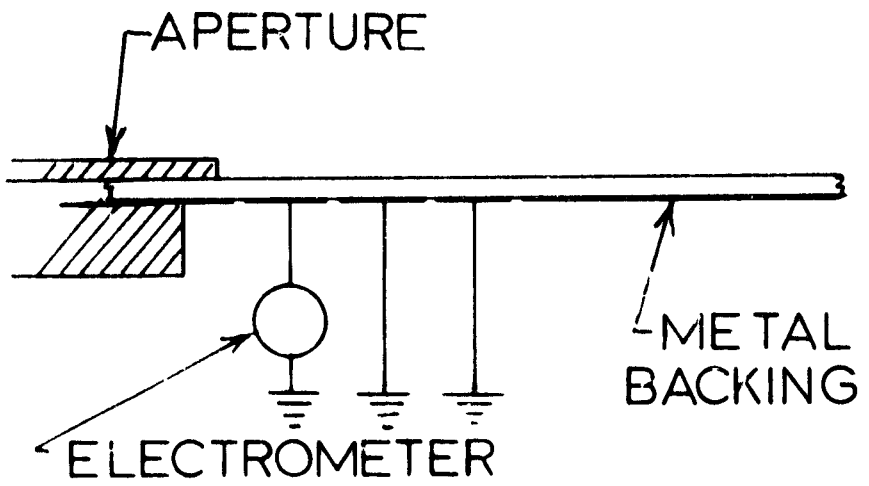

Figure 1. Schematic diagram showing a dielectric film and its segmented metal backing. The aperture plate defining the edge of the specimen is also illustrated.

Some limiting factors need to be noted. One of these is that determining the surface potential requires knowing the capacitance between each segment and the adjacent area on the dielectric surface. Though this can be measured and calculated, the accuracy of this method is not as great as other methods yield. Also this method suffers from lack of resolution in that the minimum size of segment which was practical was about 1 mm, this with hand construction. Use of photolithographic techniques might improve resolution.

The principle value of this method is that it yields results quickly and with little data processing. The measurement of charge on one segment can be converted to surface potential

directly above that segment with little regard for potential on neighboring segments, whereas measurements with beams often require extensive data processing. If charges were induced on segments located some distance from the specimen, say above the specimen, then the charge on any one segment would depend upon the potentials from many areas of the specimen. In such a case the advantage of this method would be lost.

2.3 High-Energy Charged Beams

High energy implies that the kinetic energy of the particles greatly exceeds the electrostatic potentials in the region of the investigation. Thus the charged particles travel in nearly straight lines, suffering little change in speed or direction. In this case one obtains information about the region by measuring either of the changes. Though the change of speed can, in concept, be measured, and will be proportional to the integral of the electric field parallel to the path, the easier measurement by far is the deflection of the beam caused by the integral of the normal electric field. This review is restricted to measurements of deflection.

When a beam is directed more-or-less normally toward a specimen, it will deflect if there is a field parallel to the surface of the specimen. Such an effect is useful but is probably better implemented with low energy beams.

The major emphasis of this section is thus the measurement of the deflections of nonimpacting beams, examples being found in

the literature.[8] [9] [10] These methods are all based upon an assumption of azimuthal symmetry such that potential depends upon radius but not angle about some axis. Under this restriction, Black and Robinson [9] measured potential differences typically of 1kV using an 84.2-keV beam of beta particles from Cd_{109} and a detector which had a window 0.5-mm wide. Ham and Robinson [10] using beams of a few kilovolts could resolve potential differences of ten volts. Though the techniques have been used for the symmetric case, there is a possibility of extending them to other cases. Such development work could pay useful dividends in certain cases but, even without that, these methods have applications. Fig. 2 illustrates the formation of a sheath in the vicinity of some structure and the use of nonimpacting, high-energy beams for measuring the size of the sheath and also its

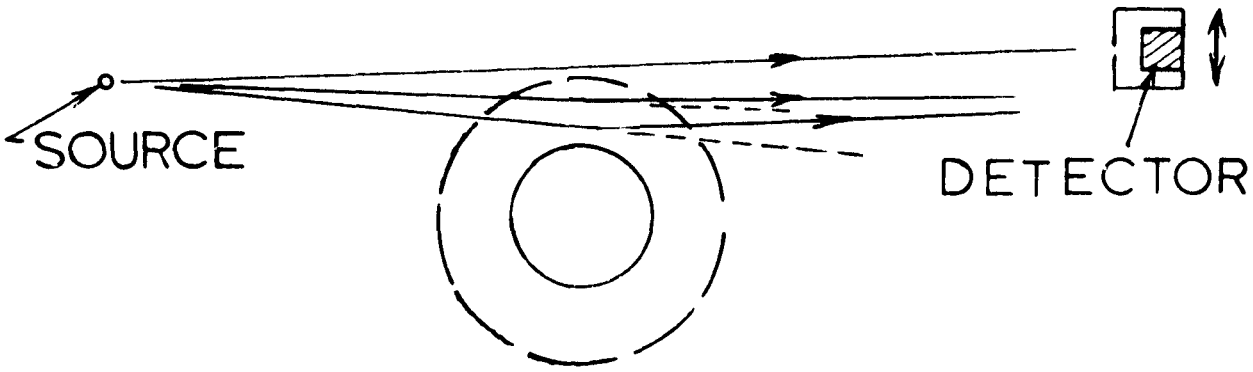

Figure 2. Scheme for measuring sheath size and potential distribution with data from deflected beams.

potential distribution.

The methods of high-energy beams have several advantages.

The data are relatively easy to collect and process. The test particles have energies (in eV) which are much higher than typical system voltages or energies of particles which might be in a surrounding plasma; consequently the test particles are easily distinguished from the others and they have relatively long mean free paths. The principal difficulty is that when an axis of symmetry cannot be identified, then the known algorithms do not apply and analysis becomes more difficult.

2.4 Low-Energy Charged Beams

When a low-energy beam of particles is injected into a region of interest it might be reflected to nearly any point on the periphery and it might also strike the specimen. One doing such an experiment needs to provide a detector for the beam at any point where its detection would provide useful information. The interpretation of data is difficult except for certain types of measurements. In this section various options in the use of these beams are described and compared.

When it is allowed that a beam may strike a specimen, then very precise measurements of surface potential are possible, and with relatively little work. The basis for such a measurement is that a beam cannot strike unless its energy exceeds the surface potential at the point of impact. The strategy is to choose a beam energy known to be too low and to direct a short pulse of electrons toward the surface. Then the energy of subsequent electron pulses is increased in small monotonic steps until the surface is struck. In making such a measurement the experimenter

must be able to detect when that occurs, typically by observing induced charges in the metal substrate. If the direction of impact is normal, then the potential of the surface is known to lie between the energies for the first test causing a strike and the preceding test.

Generally the beams will impact obliquely unless special efforts are made to calculate where the electron beam source should be located. Iterative procedures and trajectory simulations[11] can be used together to locate these injection points and calculate trajectories leading from those points to corresponding points on the surface of the specimen. One must solve a self-consistent problem of calculating trajectories from the potential profile which in turn is being formulated in terms of trajectory data.

In a more ideal sense, trajectories would not strike but come arbitrarily close to the surface. From a knowledge of initial conditions for each trajectory and from a measurement of end points, one would hope to calculate the potential distribution to whatever accuracy is desired by choosing a sufficient number of trajectories. Yet the choice of trajectories is not arbitrary. Tilley[12] has shown that iterative procedures for interpreting data can lead to grossly inaccurate results, possibly because of ambiguity in the data, but also possibly from an ill-conditioned process. When data are selected properly, then the process he developed converges to a reasonable estimate.

The use of low-energy particles depends upon having an

accurate and economical simulation; one can hardly be evaluated without the other. Also the procedure depends heavily upon the geometry. Specific cases will be discussed in later chapters. Though low-energy beams may be preferred for impacting measurements, the use of high-energy beams is inviting otherwise. The reason is that the latter beams deflect very little from their unperturbed trajectories, and thus that the number of iterations can be kept small.

2.5 Ion Production

A technique quite different from the others is to create ions in the region of interest, to allow them to drift out of the region, and to detect them as they leave. These ions would have negligible kinetic energy where they are formed and would gain energy equivalent to the difference in potential between the source point and the detector. Thus a measurement of energy at the detector would be equivalent to a measurement of the source point potential. This technique has been described in reports by Ross[13] and also by Robinson.[14] As described in those reports, the method was not very satisfactory because of the small signals involved and the lack of resolution. The means of ionizing particles was a collimated beam, either electrons or photons, which was steered to the precise point of interest. Also the neutral gas density had to be large enough to provide a signal without being so large as to influence the system under test. The constraints prevented this system from being as practical as the others which have been mentioned.

2.6 Combination of Techniques

The use of both impacting and non-impacting beams can provide the benefits of both types of measurements. The high precision of the impacting measurement provides the potential distribution on a surface, but when plasmas are present, the potential distribution in the neighboring region depends upon the sheath as well. The nonimpacting measurement yields information about the region through which the test beams pass and complements measurements made directly on the surface. Of course one must use a model of the sheath to predict where impacting beams will strike and, on the other hand, one conveniently uses surface data to set the boundary conditions of the sheath.

A possible diagnostic system would thus have two sources of electron beams. One would be a low-voltage source which would direct electrons toward the surface for impacting measurements. The other would be a high-voltage source set on one side or the other of the test specimen such that it could direct electrons in a path passing near to but approximately parallel to the surface. The two have complementary roles, especially important if plasma is present, yet together they do not resolve well in the dimension parallel to the surface. Segmenting of the substrate provides the necessary reference locations on the surface.

3. SIMULATION OF POTENTIALS AND ITERATIVE CALCULATIONS

Although several methods of measuring potential are evident from the previous chapter, most of these methods require supplementary calculations for their interpretation. The user does not merely want to know the outcome of a particular trajectory, but he wants to predict the outcome of any trajectory from a relatively small subset of measurements. His need is then to construct a self-consistent model which matches his actual measurements and which can be used to predict other trajectories. A poor choice of experimental data or a poor choice of model could result in long calculations or unreliable modelling. The advantages and disadvantages of several models are presented in this chapter.

3.1 General Features of a Model

Any model must have certain features. It must fit the constraints of the physical system and it must provide values of electric field and potential at points on the surface of the dielectric specimen and in regions near it. The work which has been done has been for conditions where Laplace's equation holds near the specimen, which is to say that space charge is neglected. Such an assumption greatly simplifies the work. However possible extensions to cases with space charge will be noted in the following presentation.

Two interrelated processes dominate the problem at hand. First of all, one needs to know the potential distribution to calculate trajectories. That first process is relatively simple

and easily programmed. However the potential is not known at the outset so that it must be assumed. Consequently the second problem is that of iteratively improving the potential function to reduce the discrepancy between measured and simulated trajectories. This latter problem is not well understood. It depends on the choice of model as well as the method of measurement. Finding a model which matches a set of measurements is no guarantee of accuracy. The iterative process may converge to unrealistic potentials if the trajectories are not carefully chosen.

The general procedure is then to construct a mathematical model of potential which depends upon relatively few parameters and to calculate trajectories based upon that model. The model parameters are then adjusted to improve the match between simulated and measured trajectories. All modelling has been restricted to two-dimensions, some models depending upon conformal mapping and being restricted to two dimensions, some being used in two dimensions only to avoid complexity.

3.2 Piecewise Linear Model of Potential

Quoc-Nguyen[15] applied the techniques of conformal mapping to finding potential near a surface where potential was specified as a piecewise linear function. Dielectric surface potential had been determined from measurements of charge induced on a segmented substrate, and that potential was represented by a piecewise linear function of the distance from a metal-dielectric interface. Such an interface and the resulting potential

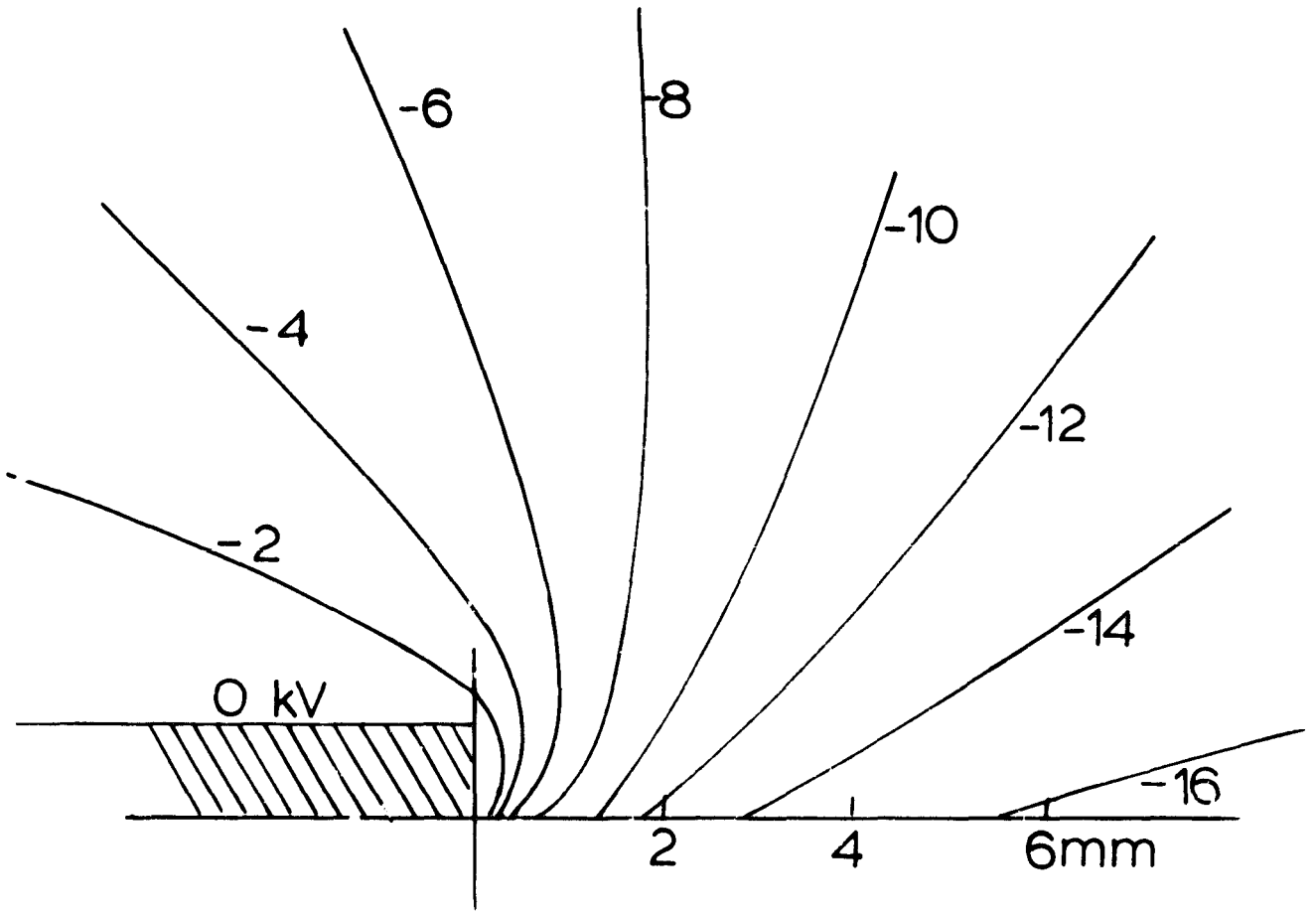

Figure 3. Equipotential contours near a FEP-Teflon surface charged in a 20-kV beam. Dimensions are in mm. [15]

contours are shown in Fig. 3 taken from Quoc-Nguyen. In this model the parameters are the discrete points on the surface where the potential is specified. The model is especially useful where measurements are made at discrete points on the surface, measurements such as those with segmented ground planes or with impacting beams. The model is relatively efficient computationally, but it introduces irregular behavior near the breakpoints of the potential function. The particular realization by Quoc-Nguyen converted the region of interest to the upper-half-plane by a conformal mapping and then assumed that the upper-half-plane was bounded by zero potential at infinity. Potential near the surface was found by use of a Green's integral taken over the surface. Space charge was ignored and the conformal mapping restricted the method to two dimensions.

Whereas this method is useful if measurements are made at specific points on the surface, it relies on a large number of parameters which must be set. Consequently it is less attractive for measurements which cannot be identified with specific spots, measurements made, for example, with nonimpacting beams. For this reason alternative models were sought.

A possible extension of this model is the use of a spline[16] to represent the potential on the surface. A series of measured points would form the basis for computing the spline coefficients, and for such a simulation, there would be no discontinuities as there are for the piecewise linear model. However the evaluation of potential in the region near the

surface would be more difficult.

3.3 Multipole Model

Whereas the previously discussed model emphasized points on the surface, this model is most appropriate for systems where surface impact never occurs. Tilley [12] modelled potential as the sum of potentials from many multipoles placed at appropriate points outside of the region of interest. This method, though not restricted to two dimensions by any fundamental limitation, was applied to two dimensional systems. A significant constraint is that it cannot account for the effects of space charge, should any be present, because it allows multipoles to be placed only outside of the region of interest.

The boundary potentials are never explicitly identified by this method but only as extrapolations from the regions where nonimpacting beams can pass. Fig. 4 illustrates one of Tilley's examples where the potential lines have been iteratively generated from numerical data representing the trajectory endpoints. The trajectory with the greatest horizontal displacement was important for this example, because without it, the iteration would have generated erroneous potential profiles.

The method as it was realized required substantial computer time, and it was restricted to simple geometries, parallel planes or cylinders, where image theory could be used. Also the lack of explicit surface potentials made it undesirable for studying secondary emission, a process involving surface impact. Though

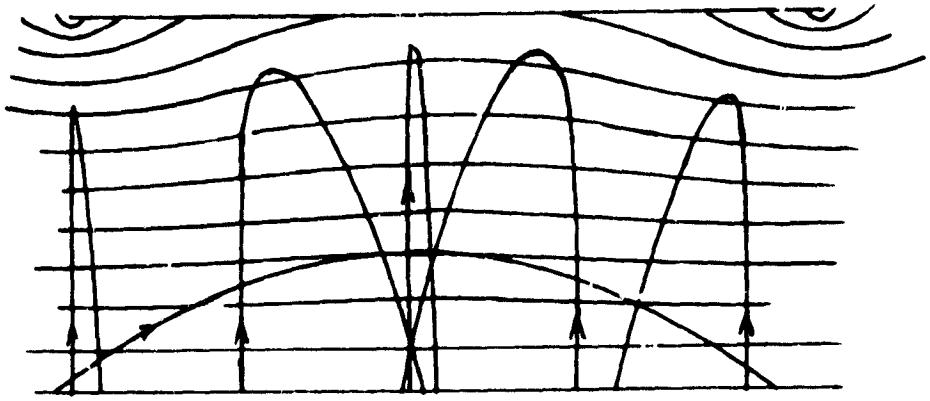

Figure 4. Example of potential contours iteratively generated to match particle trajectories.[12]

there might be unrealized benefits in this method, it was displaced by the next method to be described, a method specifying surface potential with a small number of parameters.

3.4 Polynomial Model

An experimental system was built expressly for the purpose of measuring secondary emission and it was built in such a way that detailed simulations could be done. This system and its use have been described in various ways by Robinson and Budd,[17] by Budd,[18] by Javidi,[11] and by Robinson.[19]

This system, which uses a polynomial representation of potential on the surface of the specimen, has been described in detail and will be mentioned only briefly here. The heart of the experimental system is a flat dielectric specimen mounted on a

plate which lies on the axis of a metal cylinder. Both the plate and the cylinder rotate but such that the dielectric specimen always faces a region of space bounded by the cylinder walls and the mounting plate itself. This chamber, represented as a half-cylinder, can be changed to a half plane by a conformal mapping. Consequently the potential can be calculated with a Green's integral as discussed previously. The potential on the specimen is represented by an expression of the form

$$V = V_o \{1-(X/B)^n\}, \qquad (1)$$

or perhaps by an expression with more terms, where X is the coordinate measured along the surface from the center of the specimen and B represents the edge of the specimen. This representation is made in the upper-half-plane obtained by the conformal mapping.

The expression for the potential contains the constant V_o which is merely the potential at the center of the specimen. This quantity is easily and precisely measured by allowing test beams to strike the certer of the specimen, as described in the previous chapter. The exponent n is then estimated by selecting it for a best fit with trajectories deflecting from the surface. Generally smaller values of n are used with larger values of V_o. Budd[18] illustrates this relationship.

The polynomial model has been used extensively for interpreting measurements of secondary emission in the half-cylindrical test system. Consequently several features of predicted trajectories are illustrated here and a consistency

check with experiment is also made. Measurements in the center of the specimen are less complicated than measurements near the edge so the illustrations given here concentrate on the edge region. The specimen itself is considered to lie on the horizontal axis of a coordinate system, reaching between the limits $-3.17mm < x < 3.17mm$ with $y=0$. A small portion of the specimen is represented by the horizontal axis of Fig. 5. For this figure the center of the specimen at $x=0$ is at 10.1kV and the edges are at 0kV. Test beams approach the specimen with different initial energies and from different angles. These beams strike with specific angles and impact points or they may deflect away from the surface. Because the surface potential is not uniform, beams with high energies can impact in regions which lower-energy beams cannot reach. Although the figure shows single-line trajectories the beam itself has a width of 0.15mm and more appropriately should be considered as a bundle of trajectories of the type shown.

Each of the two families of curves shown in the figure corresponds to a specific injection point and specific energy but within each family the beams differ in that they have been deflected as they entered the test chamber. Many other options exist and they can be summarized with graphs such as shown in Fig. 6. For this graph the abcissa is the impact point of the beam and the ordinate shows the angle at which the beam impacts the dielectric surface. Each of several curves can be identified with a beam energy and an angle θ which defines the point of injection. The various points on each curve represent different

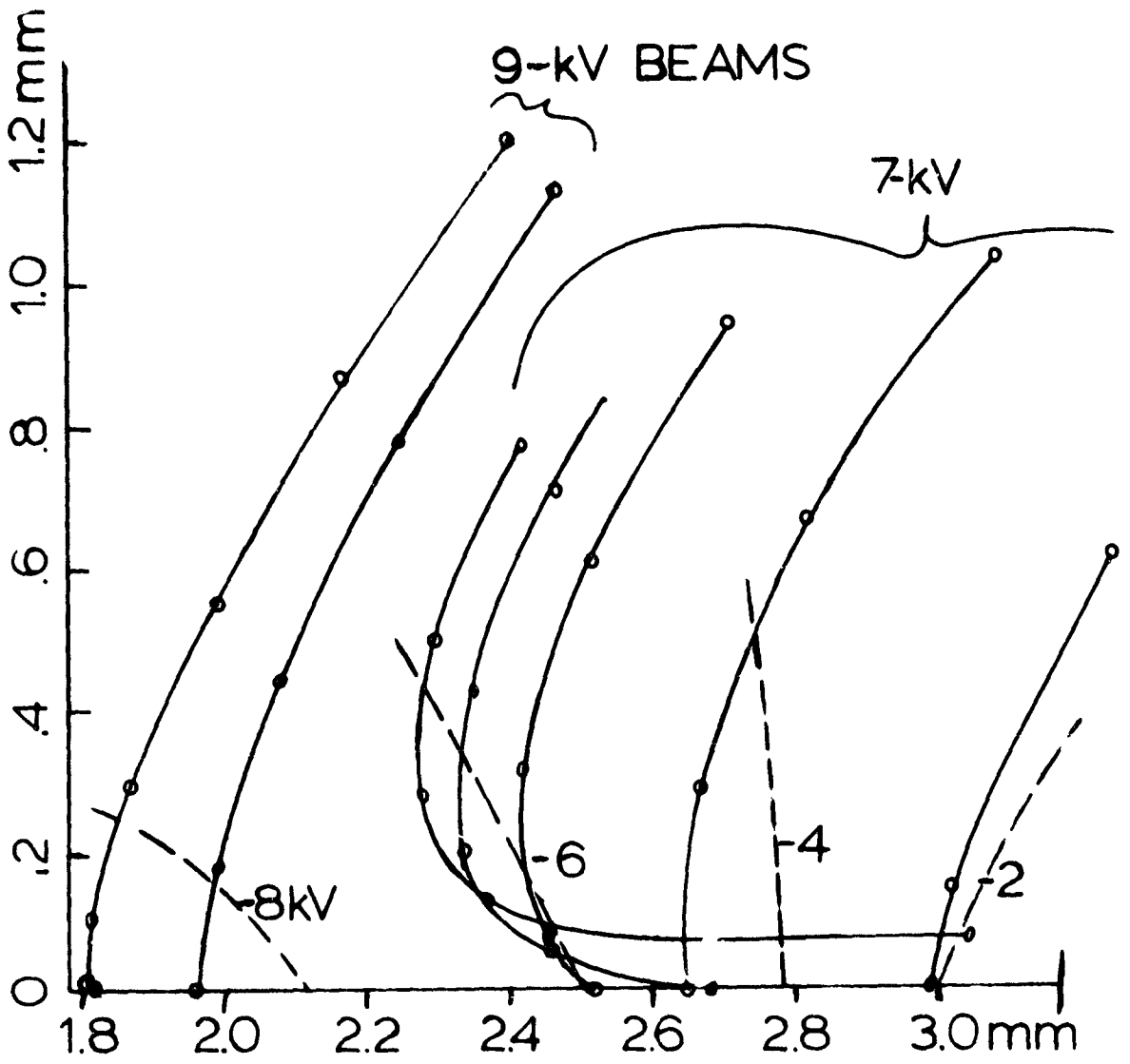

Figure 5. Typical trajectories near the surface of the dielectric specimen as simulated by the model using a polynomial to represent potential on the surface. Equipotential contours are shown with dashed lines.

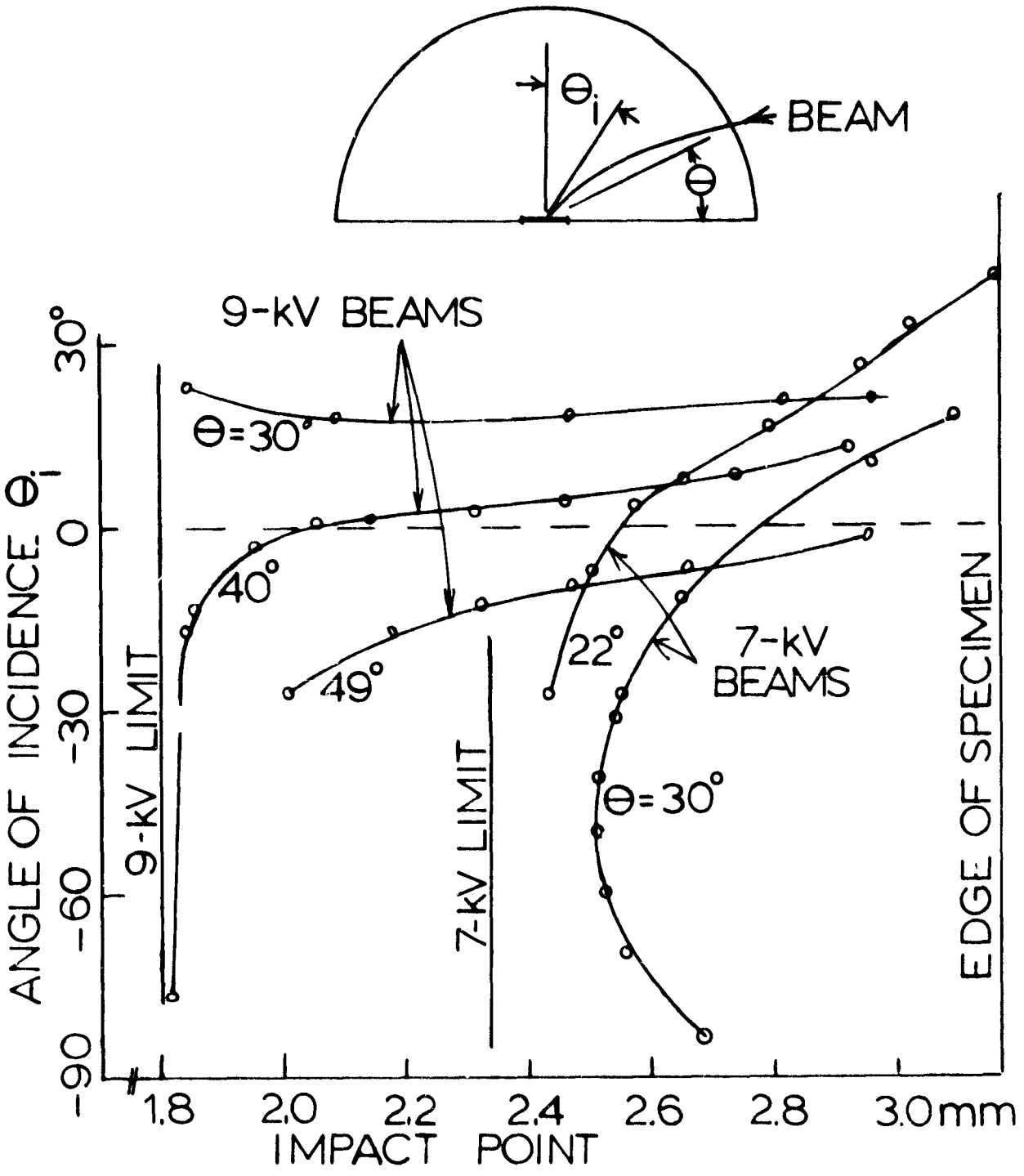

Figure 6. Summary of impact conditions for various beam injection parameters. The potential at the center of the specimen is 10.1kV.

deflection angles. The allowable ranges are identified for the particles with either 7 or 9kV of energy and the edge of the specimen is also marked. One curve that is of special interest is that corresponding to 9kV and 40 degrees. For this curve the impact angle is very close to normal over a wide range of impact points.

Though the two previous figures show only simulated values, a useful check may be made with experimental data.[20] Let us consider for example the curve for 9kV and 40 degrees shown in Fig. 5. Review of the simulation shows that the deflection plate voltage for the beam to be at the left-hand limit is -95V whereas the voltage for the beam to strike the right-hand limit, or edge of specimen, is +95V. The deflection plate voltages actually measured which produced these two conditions were -105 and +85V. Even though a shift occurred, the range in deflection plate voltages was the same for the simulation as for the measurements. For the case with 7kV and 30 degrees, the simulated values were -135 and -20; measured values were -130 and -10V. Though a check such as this does not guarantee accuracy it supports the use of the model derived from other measurements.

3.5 Models With Azimuthal Symmetry

Whenever an axis of rotation can be identified, then the surface of interest has a potential which is a function only of cylindrical coordinates r and z. Let us consider that high-velocity probing beams have measurable deflections in the r-θ

plane. Trajectories having different impact parameters (radii) deflect at different angles, and this type of data can be used to calculate potential as a function of radius, for some z. Thus one may generate maps of potential vs r and z. If no space charge is present and if the surface is a smooth cylinder or sphere, the problem is trivial, but more generally this method can accomodate space charge as well as z-variations. This method is well suited to identifying sheath sizes around objects such as probes or booms.

As with any method of measuring potential, the spacial resolution must be sufficient for the application. If sheath sizes are equal to or less than the width of the probing beam then measurements cannot be made. However if sheath sizes are small, upper limits upon their size may be placed by measuring the surface potentials with direct impact and then demonstrating that such potentials do not exist beyond the minimum distance for which nonimpacting measurements are possible.

3.6 Inclusion of Space Charge

The work conducted on this grant has been for situations where space charge was not important, and thus, the limitations of the various methods with respect to space charge were not important. Yet other situations might well call for the use of similar techniques if they could be adapted for use with space charge. Several approaches are possible.

In the previous section it was noted that space charge was

easily included. The method described there uses sequences of trajectories which are closely spaced and which yield values of potential at those points through which the trajectories pass. No functional expressions are used for the modelling.

However when models depend upon a description of the potential on the boundary, then neighboring potentials cannot be predicted from that surface data by itself. Then one might extend the models by defining exponential functions of distance from the surface. These functions, depending upon a small number of parameters, might reasonably represent potentials near surfaces so that trajectories could be simulated. One should not pursue this approach very far without considering the elaborate numerical modelling represented by NASCAP.[21]

A third way of handling space charge is to place charges in the region itself and to evaluate their effects with a different type of Green's integral. Presumably one would first measure and carefully define the surface potentials with some method such as beam impact. The effect of the surface potential on trajectories would be computed and found inadequate to describe observed trajectories. Thus space charge distribution functions could be manufactured to achieve the desired agreement between measured trajectories and those predicted from the model.

The experimentalist is interested primarily in specifying potentials in regions of interest. The model is not as important as the precision and extent of the measurements, and models which might be developed would not necessarily be compatible with

theoretical constructs. Consequently methods such as the first, which merely yield values at specific points, may be better than those which attempt to adjust parameters in a model. However, for the more complex potential contours, parametric modelling may allow one to specify the potential contours with relatively few measurements, yet with loss of detail and accuracy.

4. MEASUREMENT OF SECONDARY EMISSION COEFFICIENT

The process of recording a secondary emission coefficient is relatively simple; the resulting number must then be associated with impact point, impact velocity, and impact angle if it is to be meaningful. The previously discussed simulations provide a way of determining the associated parameters.

Measurements have been made for 5-mil (0.127-mm) FEP-Teflon which has been backed with a metal coating maintained at ground potential. The measurements and associated parameters are summarized in this chapter.

4.1 Principle of Induced Substrate Charge

The secondary emission coefficient is defined as the ratio of all electrons leaving a surface to the number of primary electrons which strike the surface. This definition does not distinguish between various types of secondaries, those with low energy sometimes referred to as true secondaries, and those with high energy known as backscattered electrons. The number of high-energy secondaries is a relatively small fraction of the total for the cases of interest in this work and no attempt is made to correct the experimental data before comparisons are made with low energy theories.

The definition which is used is compatible with the method of measurement. When a pulse of electrons strikes a surface and electrons are given off, the change in the number of electrons on the surface depends upon the secondary emission coefficient. The

surface of the dielectric is strongly coupled to the underlying grounded coating by the capacitance of the dielectric film. Because this capacitance dominates other capacitances, the charge induced in the metal is approximately the same as the surface charge. Thus a measurement of the charge induced in the metal when primary electrons strike the surface provides a means of calculating the coefficient, a means which does not discriminate among the energies of the escaping particles.

Let us suppose that a pulse of electrons having charge q_p strikes a location of the specimen and that some change q_d is observed in the substrate. This change is the difference between primaries and secondaries where the secondary pulse is designated q_s. The secondary emission coefficient henceforth designated σ can then be calculated as follows:

$$\sigma = \frac{q_s}{q_p} = \frac{q_p - q_d}{q_p} \qquad (2)$$

Finding the coefficient requires two measurements, the primary charge which is determined with a Faraday cup and the change in the substrate charge.

The specimen is assumed to be nonconductive so that the change in surface charge represents a change in the surface potential. Yet for the measurement to be meaningful it must be made at a specific surface potential. Consequently the amount of charge deposited must be limited by the allowed change of potential. For certain cases q_d is small compared with q_p and the criteria is applied to the difference, not the primary

charge. Thus for these cases, higher than usual values of q_p may be used. The value of q_p depends not only on the allowed change in potential but also on the area impacted. The use of a larger area allows the use of larger pulses but at the same time reduces the spacial resolution which may be achieved.

4.2 Transient Response to Step Function

The work of Quoc-Nguyen[15] was done with an experimental system where the primary electron beam could not be pulsed. Nevertheless he was able to insert a mechanical shutter in his system and measure the effect of electric field upon the critical energy corresponding to $\sigma = 1$. His measurements were of the transient currents induced in the metal coating when the electron beam, withheld by the shutter, was allowed to strike the specimen. At the time when the transient was initiated, the dielectric surface was at a known charge state, the state for which measurements were sought. At time zero when the beam first struck the specimen, the response was as desired, but it changed with time. By extrapolating backwards and accounting for the pass band of the instrument, Quoc-Nguyen was able to estimate the response at time zero and thus to calculate the secondary emission coefficient. Fig. (7) taken from his work illustrates how electric field normal to the surface of the specimen affects the coefficient. Note that all curves correspond to a coefficient of unity when $E_p = 0$. The most accurate measured feature of the curves is the location of the left-hand intercept with unity. As surface electric field is increased, the point

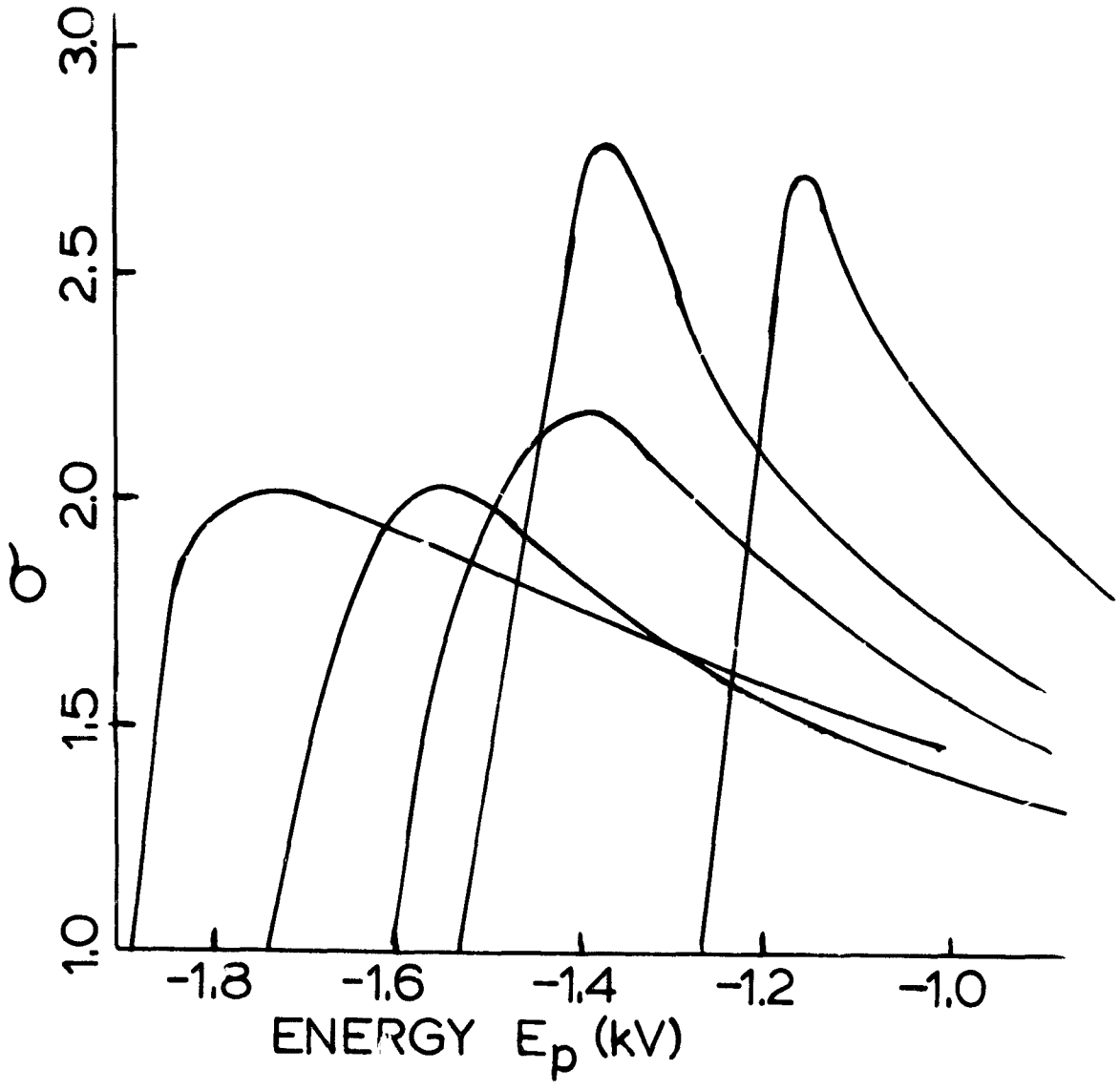

Figure 7. Secondary emission coefficient as a function of energy of the impacting beam. In this plot, the energy is shown relative to the energy of the impacting electrons which originally charged the surface. All curves have a common point at $\sigma = 1$ and $E_p = 0$. The peaks as ordered from right to left correspond to curves measured at various normal electric field strengths ranging from 0.3 to 3 MV/m. [15]

shifts progressively to the left.

4.3 Transient Response to Impulse Function

Budd [18] and Javidi [11] have refined the measurements made by Quoc-Nguyen and they have extended them in several ways. They used a system which was designed specifically for secondary measurements and which had a pulsed beam for making measurements. The specific parameters of the new system are described in this section.

The electron beam was collimated with slits so that it struck an area of the specimen about $0.15 \times 1 mm^2$. This small size was chosen so as to resolve details over the 6-mm width of the specimen.

The critical energy was typically between 1.5 and 2 kV such that changes in σ could be observed when surface potential changed on the order of 200V. If the capacitance is found by using a dielectric constant of 2.1, then it may be used to find the allowable charge deposition:

$$dq = C\,dv = (150 nF/m^2)\,(200V) = 0.03\ mC/m^2. \qquad (3)$$

When the area struck by the beam is included, then the allowable change in surface charge is about 5pC. Such a small charge was near the resolution limit of the instruments being used, but more important was near the noise limit, noise coming not from the instruments but from the experiment itself. Measurements were generally made at or below this value, with there being a constant effort to find a reasonable compromise between the

various conditions. Measurements below 1pC were possible under many of the conditions investigated.

All measurements made with this system were tracable to Faraday cup measurements of the primary pulse. However, finding a place for the cup was difficult. Budd [18] used a removable cup, calibrating the beam and using secondary emission from an uncharged surface as a secondary standard. Javidi [11] built two different cups which could be permanently mounted, but found one to be inaccurate because of its location. His better cup was attached to the rotating cylinder facing outward so that it could be positioned near to or under the orifice of the beam. This cup was then used for direct calibration of the beam during measurements.

If the beam is to transfer a pulse of 5pC, it can be of various lengths and currents. For this system, both users chose pulses of about 20ms so that the beam current would then be 0.25nA. Such a low current was considered to have inconsequential space charge and it was easy to produce. On occasion, the time of the pulse was made much longer, say 2s, when the charge q_d was much smaller than q_p. The 20ms beam was sufficiently short that it appeared as an impulse driving function for the electrometer which monitored the experiment. Thus the response of the electrometer, set to measure charge, was a step function whose risetime was limited by lowpass filtering.

4.4 Normal Incidence and Normal Field

Quoc-Nguyen,[15] Budd,[18] and Javidi[11] have all made measurements for these conditions and their results are compared in this section. Though Budd and Javidi used similar systems, Quoc-Nguyen's was significantly different. He used circular specimens having diameters from 2.5 to 5cm which were considerably larger than the 6-mm strips used by the other two. Furthermore Quoc-Nguyen controlled field strength at the surface of the specimen by placing a fine-meshed wire screen at various distances above the surface of the specimen. The others placed the specimen in a much smaller chamber and relied solely of the specimen's charge alone to produce the fields.

Measurements in a region of normal field require that the measurements be at the center of the specimen. All systems could be operated in this way with the test beams striking normal to the surface. Note that all surfaces were charged prior to making measurements and the surface charge came to a steady state during the charging process. This steady state is reached when the critical energy for secondary emission is precisely the difference between the surface potential and the energy of the electrons which flood the surface during charging. Thus one can determine the critical energy merely by measuring the surface potential and the original flood gun voltage. Figure 8 taken from Quoc-Nguyen summarizes his results. Budd and Javidi both demonstrated a low-field limiting value of 1.5kV for an uncharged specimen, this being shown on Fig. 8 also. Furthermore Budd

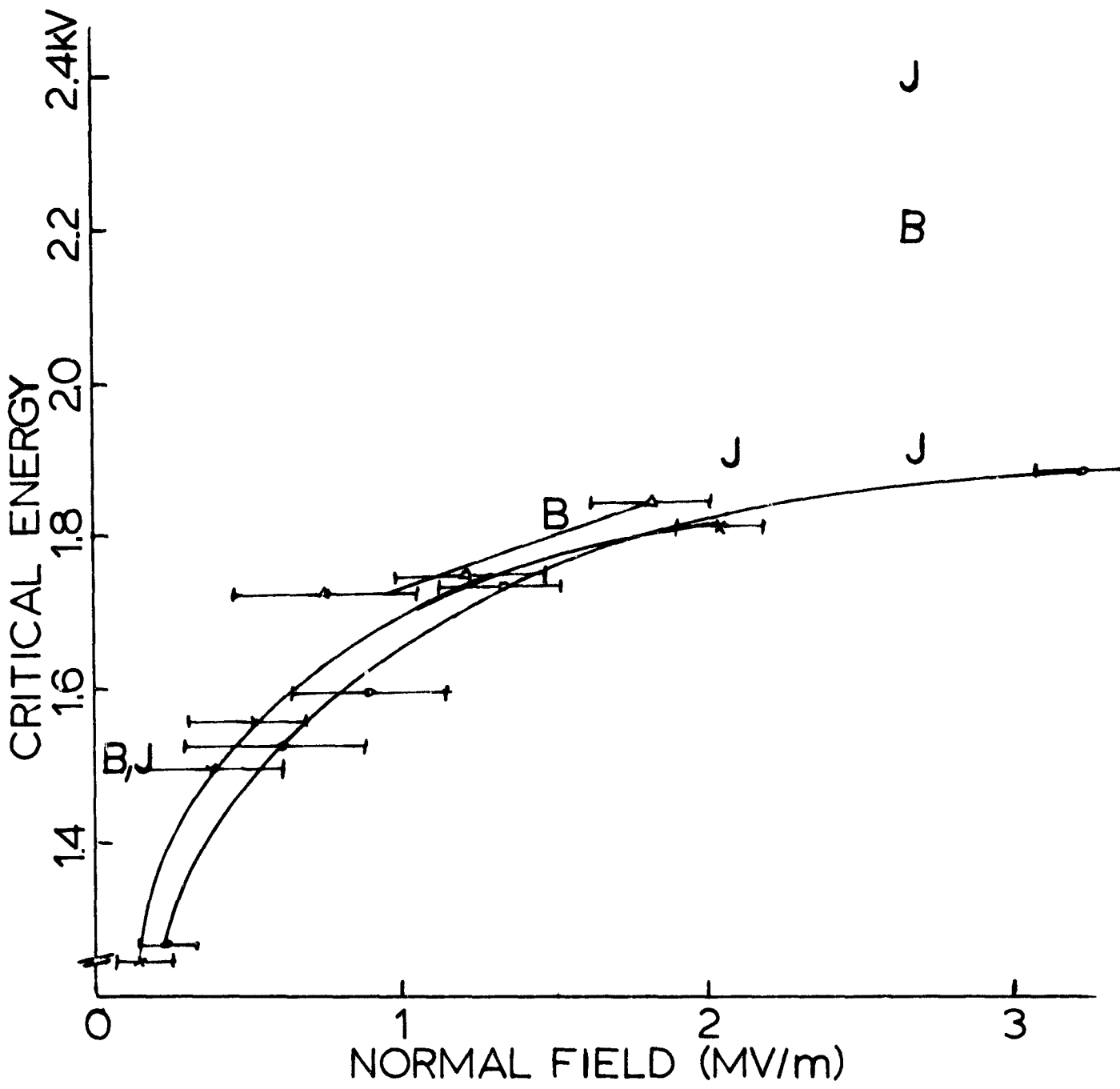

Figure 8. Quoc-Nguyen's measurements [15] of critical energy at various field strengths with superimposed values from Budd [18] and Javidi [11] identified with symbols B and J.

identified values at 1.5 and 2.7MV/m while Javidi measured different values at 2.7 corresponding to different lengths of time under vacuum. The figure shows that Quoc-Nguyen's measured values were somewhat lower than the others but that all found similar trends. Quoc-Nguyen's measurements of field strength were relatively crude and thus preference should be given to the other measurements. Yet the low field limits do not agree and thus the discrepancies cannot be attributed solely to the measurements of field strength. Nguyen's specimens were in vacuum for shorter periods of time than for the others, and as Javidi's results indicate, the value of critical energy tends to increase with time. Javidi's result at 2.4 kV corresponds to a period of several months under vacuum during his testing program. Thus a possible explanation for the discrepancies is found in terms of specimen ages.

4.5 Theoretical Formulation of Secondary Emission

Various theories which have been discussed in detail [15][18][11] reduce to the form

$$\sigma = (E_o/E)^n \, (1/\cos\theta_i) \qquad (4)$$

where E_o and n are constants. The impact energy is E and the impact angle is θ_i. When normal fields are applied to the specimen both E_o and n change. Thus one would ask if the angular dependence can still be predicted by the inverse cosine function. Measurements shown in the two following sections are compared with formulas of this type where the constants have been chosen

to yield correct results for normal incidence at the center of the specimen. It should be noted that the formula applies only if E is greater than a few hundred volts, as that assumption was made to eliminate an exponential dependence from the formula.

4.6 Oblique Incidence and Normal Field

Budd's measurements [18] were taken mainly near the middle of the specimen where the electric field was normal to the specimen. Yet by tilting the specimen relative to the probing electron beam, he was able to make measurements at a variety of angles. A typical series of data was collected by setting the beam source at a specific location and then probing the specimen with beams having different deflections as they entered the test chamber. These beams would thus strike different spots on the surface of the specimen. Of course two measurements could not be made sequentially in the same spot and periodically the surface charge state would need to be refreshed.

Typical of Budd's results are those shown in Fig. 9 which was taken from his report. The theoretical curve was found by selecting parameters for a good match at normal incidence and introducing the factor $\cos^{-1}$ as described in the preceding section. At the right-hand end of the plot, the experimental trajectories skim the surface, even miss it, and thus the theoretical prediction is larger than is measured. For many different series similar behavior was found; the use of $\cos^{-1}$ provided a good match between measurements and theory. Also it

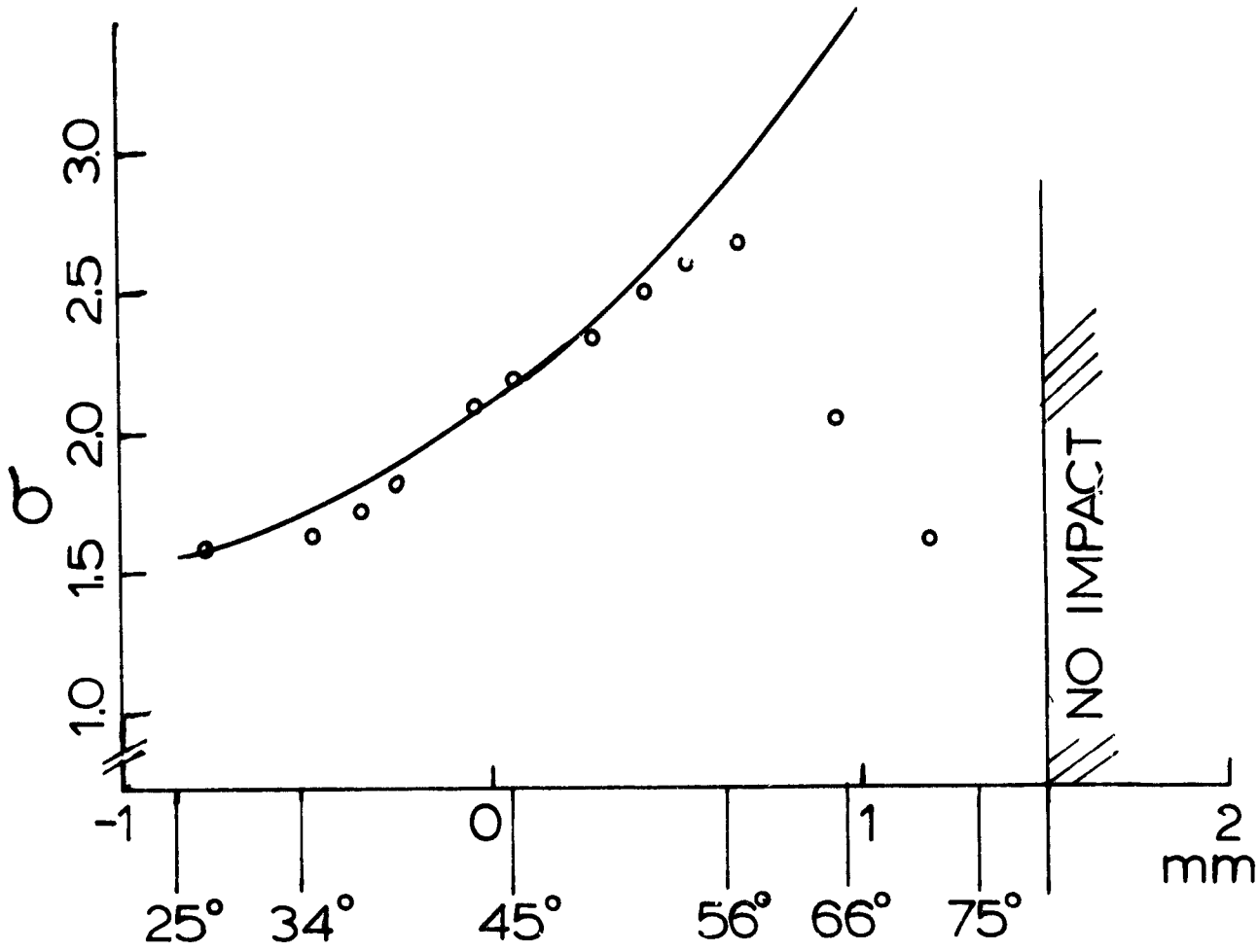

Figure 9. Budd's [18] comparison of experimental data with theory for 45-degree incidence upon a surface charged to 6.15kV. The primaries impacted with energies of 1.05keV and struck near the center of the specimen at 0mm. Specimen width was 3.17mm and angle of incidence varied about 45 as shown on the abcissa.

should be noted that Javidi's measurements near the middle of the specimen were in agreement.

The discrepancies at grazing incidence need a more careful analysis. First it should be noted that the method of measurement yields a secondary coefficient of unity if the beam misses the specimen. In case of a partial hit, a case where some but not all of the electrons strike the surface, the coefficient will be between the true value and unity. The previous statement is correct whether the true value is greater or less than unity. In cases where there is a discrepancy from theoretical predictions, one must analyze the trajectory and determine whether or not particles will all strike the specimen. This issue becomes especially critical in the next section of this report.

4.7 Oblique Field

Budd [18] made one series of measurements that showed departures from theory which could not be accounted for in terms of particles missing the targeted spot on the specimen. The measurements showing this discrepancy were near the edge of the specimen in a region where strong tangential fields occurred. The results of the series shown in the previous figure imply that particles may have missed the target in the range near 1mm. But for the case shown in Fig 10, the angles were not close to grazing incidence and the width of the beam (0.15mm) was small compared with the range over which measurements were made. Thus the argument that particles might miss the target is not

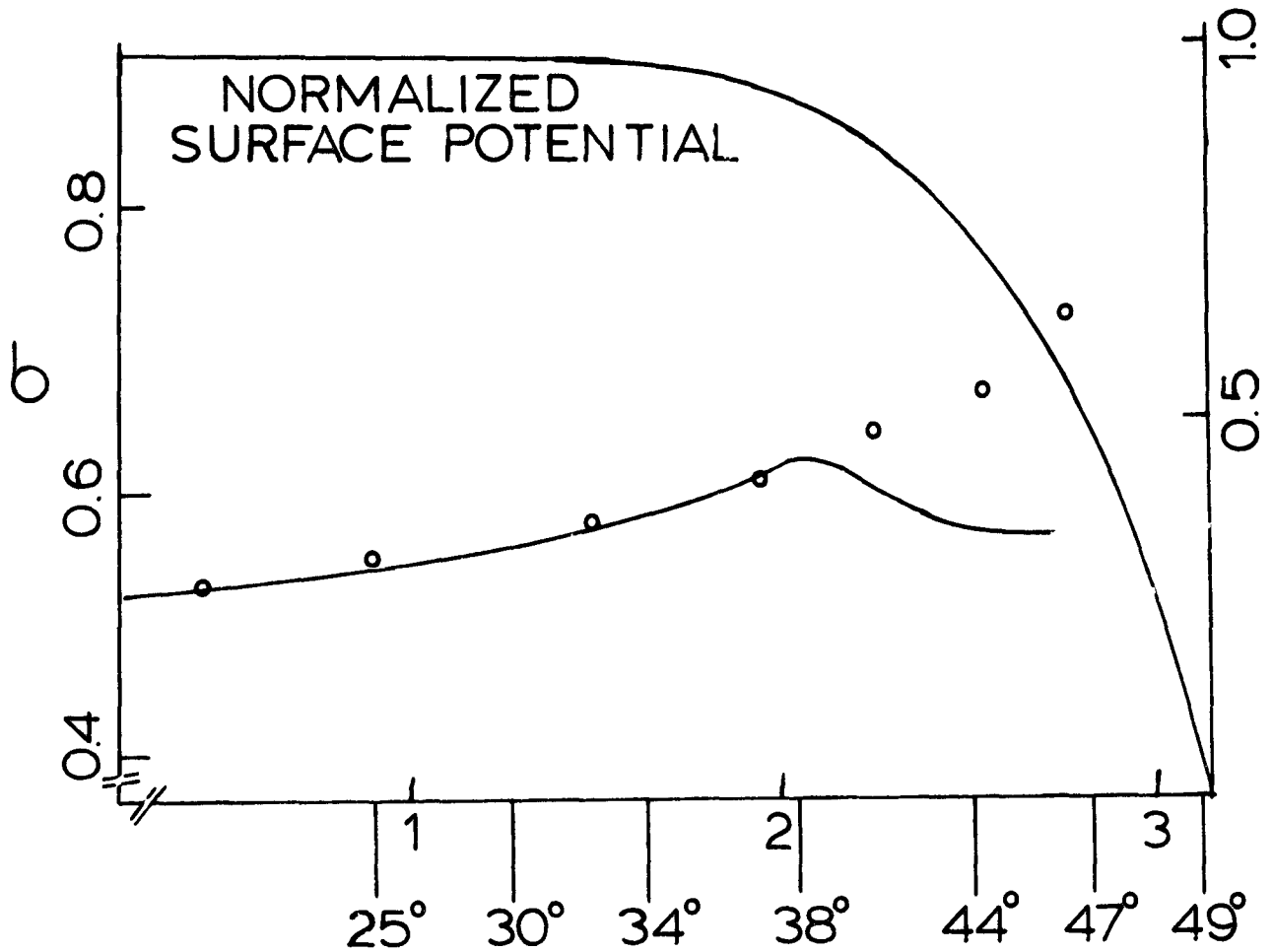

Figure 10. Budd's [18] comparison of experimental data with theory near the edge of the specimen. The center of the specimen was charged to 6.15kV and the impacting beams had been accelerated to 13kV.

supported by the simulation in this case.

Javidi's work [11] concentrated upon refining the measurements near the edge where the principal component of the electric field was tangential. The conclusion of many measurements at different energies and different angles of incidence is very simply stated, that the secondary emission coefficient approaches unity near the edge of the specimen. Figure 11 illustrates his data for the case of near-normal incidence. It must be noted in this case that any points to the left of -3mm are erroneous because the target area on the specimen is smaller than the width of the beam. Yet for data on the right of the -3mm-point, the full beam should be impacting the surface at normal incidence. Another graph from Javidi is shown in Fig. 12 where the angle of incidence lies between 20 and 40 degrees.

For both of the preceding figures the surface potential at the center of the specimen was 10.2kV and the impacting beams had initial energies as specified. The actual energy at impact is the initial energy less that lost as the beam passes through the field near the specimen. One may refer back to Fig. 5 to estimate the surface potential at the impact point and thus to calculate the impact energy.

Though the observed values of secondary emission coefficient suggest that the injected beam may not be reaching its target at full strength, the simulations do not support such a claim except within one beam width of the edge of the specimen. Certainly the

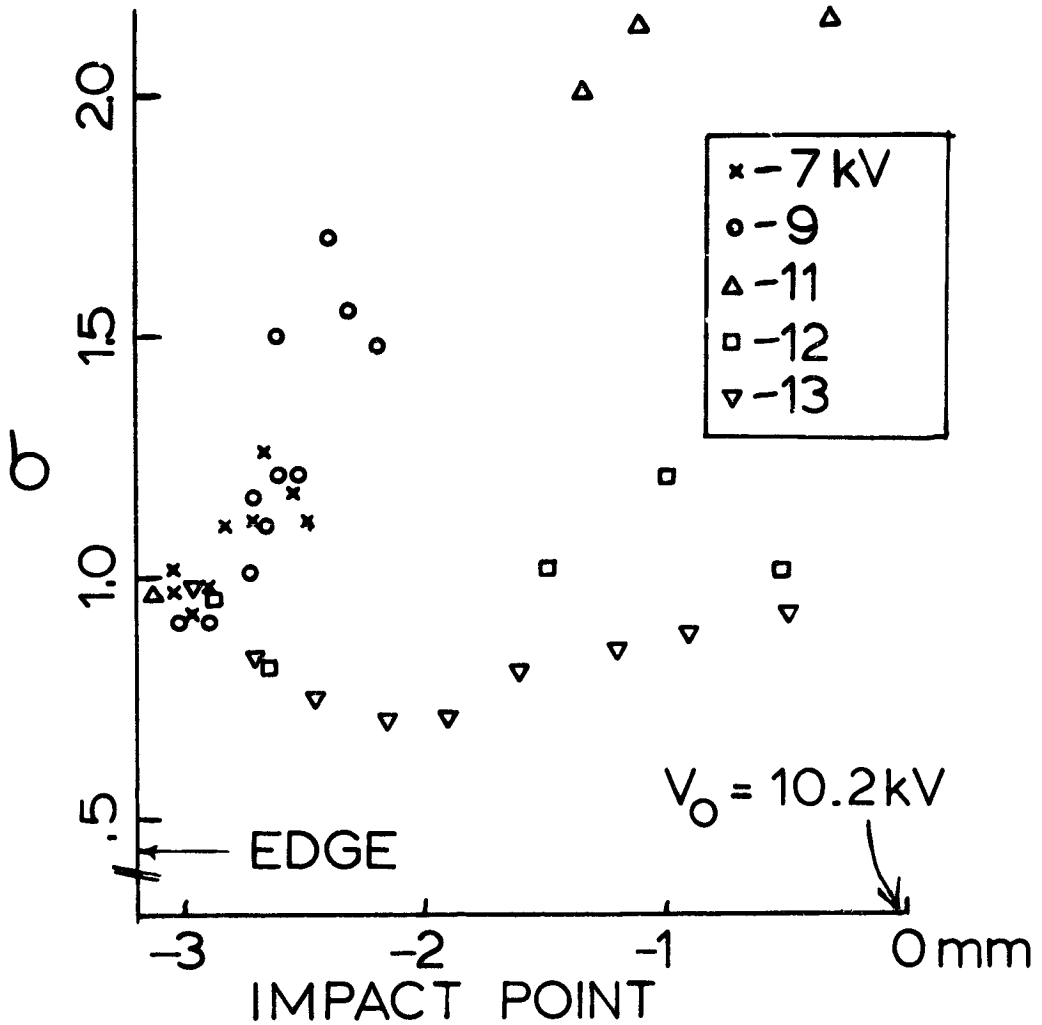

Figure 11. Javidi's [11] data for near-normal incidence near the left-hand edge of the specimen. Different symbols correspond to different impacting beam energies.

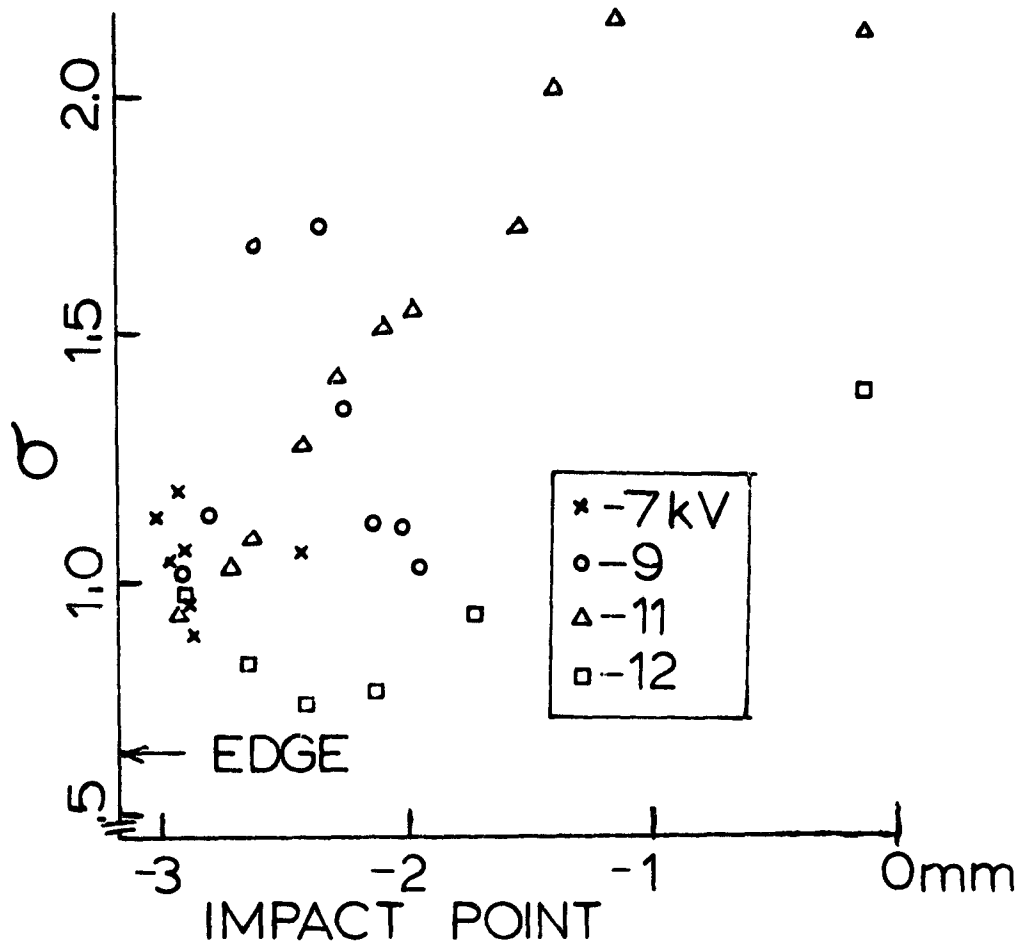

Figure 12. Javidi's [11] data for incidence between 20 and 40 degrees for various energies of impacting beams.

measured coefficients are not consistent with theoretical predictions between 2.5 and 3mm from the center of the specimen and one possible explanation might be associated with the presence of the tangential electric field in that region. The tangential field under the surface of the specimen must, by use of boundary conditions, be the same as the field above the surface and that field may indeed have some effect upon the emission process.

4.8 Extensions

Variations on the basic scheme of measuring secondary coefficient can be implemented. All measurements reported here were for symmetric distributions of charge on the surface of the specimen yet it was demonstrated by Javidi [11] that an asymmetric charge may be established by tilting the specimen while it is being charged. Measurements might be made for a variety of materials under different charge levels as long as charge does not leak off so fast as to preclude measurements. Possibly a system could be used where both charging and probing occur simultaneously, such a system to be used when charge leakage is high.

Measurements have demonstrated that electric field and aging both influence secondary emission. Existing theories do not account for these effects though empirical modifications allow the adaptation of theory to the phenomena. However the theory does not fit at all near the edge of the specimen. A theoretical investigation of how fields and buried charge layers affect

secondary emission might yield useful insights.

5. SUMMARY

Two major activities can be identified with Grant NSG-3166. The first of these is a study of various methods for measuring electrostatic potentials on and near charged dielectric surfaces. The other is the measurement of secondary electron emission from a charged dielectric surface, a phenomena which depends upon both field strength and age of the specimen.

Several different methods of measuring potentials are described in this and preceding reports. Each has advantages and disadvantages which relate to its usefulness in any given application.

The method of induced charge is relatively easy to implement though dependent upon knowledge of the coupling capacitance between the dielectric surface and the metal substrate underlying that surface. Spacial resolution is typically 1mm and this method can provide reference points for use with other measurements. Induced charge measurement is crucial for determining secondary emission coefficient.

High-energy nonimpacting beams will deflect as they pass through potential gradients and from a series of measurements, one can map the potential of the region traversed by the beams. Work not associated with this grant has shown this technique to be useful for cases with azimuthal symmetry and it is pointed out that such techniques would be useful for mapping potential about structures such as probes and booms. When the symmetry does not

exist the interpretation of data becomes more difficult and for such cases, data processing schemes would be needed. This technique works whether or not space charge is present.

Low-energy beams deflect drastically and they also suffer large changes in kinetic energy. Consequently measurement systems with those beams are more difficult to simulate and the preparation of potential maps is more difficult. However the slow beams have the advantage that they may be used for impact studies and for direct measurement of spot potentials on the surface of the dielectric specimen.

If ions are produced at some point in the region of interest, then those ions may be collected and analyzed. Their energies will correspond to the potential where they were created, and thus that potential can be determined. A lack of signal strength and poor resolution made this method less useful than the others which were studied.

The combination of both high and low-energy beams offers the advantages of both and should provide a good diagnostic capability, depending of course on one's being able to tailor the diagnostic to the geometry of the system under test. The combination is furtner enhanced by the use of a specimen with its substrate segmented so as to provide reference points.

One particular geometry, a half-cylinder, was chosen for the measurement of the secondary emission coefficient. This system was equipped with a low-energy beam-probing system such that the

beam could be used for measuring potentials and for measuring secondary emission. Of several models which could have been chosen to represent the potential in the space-charge-free region, a polynomial was selected to describe the potential on the surface of the specimen. Then the potential throughout the half-cylinder was calculated from the surface potential. With this system secondary emission could be measured at practically any point on the charged specimen and at any angle, except near grazing incidence where data was unreliable.

In the center of the specimen where the electric field lines were normal to the surface, the critical energy corresponding to unity emission increased as the field strength increased. Also the critical energy increased with the age of the specimen, it not being known what the aging process was. Aging could have been associated with time in vacuum or with exposure to electron fluxes.

Also the secondary emission coefficient varied as the theoretical prediction, as $\cos^{-1}$ of the angle of incidence. This was found to be true near the center of the specimen where field was normal.

Near the edges of the specimen where the electric field was tangential to the specimen, the correspondence between conventional theories and measurements was lost. In this region the secondary coefficient approaches unity for a wide variety of impact energies and angles. It is cautioned that the results could be misleading if for some reason the primary electron beam

does not strike the region predicted by the simulation. For some cases that can be shown to be what happens. However there are other cases where the simulations predict near-normal impact over sufficiently wide regions that a miss is not likely.

Possible extensions of this work include formulating potential models and iterative schemes to be used with both high and low-energy probing beams. Additional secondary emission measurements might be made, perhaps with asymmetric charge distributions on the surface of the specimen and with other types of dielectric. A theoretical study of secondary emission might be fruitful.

APPENDIX

Chronological Listing of Articles and Reports Grants NSG-3097 and NSG-3166

Robinson, J. W.: "Surface Charge Kinetics Near Metal-Dielectric Interfaces Exposed to Kilovolt Electron Flux", Semiannual Report, NASA Grant NSG-3097, August 1976.

Robinson, J. W.: "Charge Distributions Near Metal-Dielectric Interfaces Before and After Dielectric Surface Flashover," Proc. Spacecraft Charging Techonology Conference, NASA-TMX-73537, pp503-15, October 1976.

Robinson, J. W.: "Surface Charge Kinetics Near Metal-Dielectric Interfaces Exposed to Kilovolt Electron Flux", Semiannual Report, NASA Grant NSG-3097, February 1977.

Robinson, J. W.: "Surface Charge Kinetics Near Metal-Dielectric Interfaces Exposed to Kilovolt Electron Flux", Final Report, NASA Grant NSG-3097, September 1977.

Quoc-Nguyen, Nguyen: "Secondary Electron Emission from a Dielectric Film Subjected to an Electric Field", MS Thesis, The Pennsylvania State University, NASA-CR-155231, November 1977.

Ross, D. P.: "Ion Tracking in an Electrostatic Potential Distribution," NASA-CR-156983, May 1978.

Robinson, J. W.: "Mapping of Electrical Potential Distributions with Charged Particle Beams", Semiannual Report, NASA Grant NSG-3166, May 1978.

Robinson, J. W. and Tilley, D. G.: "Potential Mapping With Charged-Particle Beams" Spacecraft Charging Technology-1978, NASA Conf. Pub. 2071, pp606-620, November 1978.

Robinson, J. W.: "Stable Dielectric Charge Distributions from Field Enhancement of Secondary Emission", Spacecraft Charging Technology-1978, NASA Conf. Pub. 2071, pp734-736, November 1978.

Robinson, J. W. and Tilley, D. G.: "Mapping of Electrical Potential Distribution with Charged Particle Beams", Semiannual Report NASA Grant NSG-3166, November 1978.

Robinson, J. W. and Quoc-Nguyen, Nguyen: "Electric Fields and Secondary Emission Near a Dielectric-Metal Interface", IEEE Trans. Electrical Insulation 14, pp14-20, Feb. 1979.

Robinson, J. W.: "Mapping of Electrical Potential Distribution With Charged Particle Beams," NASA-CR-158713, June 1979.

Tilley, D. G.: "Dipole and Quadrupole Synthesis of Electric Potential Fields", MS Thesis, The Pennsylvania State University, NASA CR-1588550, July 1979.

Robinson, J. W. and Budd, P. A.: "Mapping of Electrical Potential Distribution With Charged Particle Beams", Semiannual Report, NASA Grant NSG-3166, March 1980.

Robinson, J. W.: "Mapping of Electrical Potential Distribution With Charged Particle Beams," Semiannual Report, NASA Grant NSG-3166, September 1980.

Robinson, J. W. and Budd, P. A.: "Oblique-Incidence Secondary Emission From Charged Dielectrics," Spacecraft Charging Technology-1980, NASA Conf. Pub. 2181, pp198-210, November 1980.

Budd, P. A.: "Secondary Electron Emission from Electrically Charged Fluorinated-Ethylene-Propylene for Normal and Non-Normal Electron Incidence," MS Thesis, The Pennsylvania State University, NASA-CR-163968, March 1981.

Robinson, James W.: "Theory and Tests of a Thermal Ion Detector Sensitive Only at Near-Normal Incidence", Technical Report, NASA Grant NSG-3166, June 1981.

Javidi, B.: "Secondary Electron Emission from a Charged Dielectric In The Presence of Normal and Oblique Electric Fields", MS Thesis, The Pennsylvania State University, Technical Report, NASA Grant NSG-3166, February 1982.

REFERENCES

1. Smylie, R. E.: "Keynote Address", Proc. Spacecraft Charging Technology Conference, NASA-TMX-73537, October 1976.

2. DeForest, S. E.: "Electrostatic Potentials Developed by ATS-5", 6th ESLAB Symposium (Grard, R. J. L.: ed.), pp263-276, Noordwijk, Netherlands, 1972.

3. Balmain, K. G. and Hirt, W.: "Dielectric Surface Discharges: Effects of Combined Low-Energy and High-Energy Incident Electrons", Spacecraft Charging Technology-1980, NASA Conf. Pub. 2182, pp115-128, November 1980.

4. Adamo, R. C. and Nanevicz, J. E.: "Preliminary Comparison of Material Charging Properties Using Single-Energy and Multienergy Electron Beams", Spacecraft Charging Technology-1980, NASA Conf. Pub. 2182, pp129-132, November 1980.

5. Robinson, J. W.: "Charge Distributions Near Metal-Dielectric Interfaces Before and After Dielectric Surface Flashover," Proc. Spacecraft Charging Techonology Conference, NASA-TMX-73537, pp503-15, October 1976.

6. Beers, B. L.; Hwang, H.; Lin, D. L.; and Pine, V. W.: "Electron Transport Model of Dielectric Charging", Spacecraft Charging Technology-1978, NASA Conf. Pub. 2071, pp209-238, November 1978.

7. Reinovsky, R. E., Glowienka, J. C., Jennings, W. C., and Hickok, R. L.: "Performance of a Feedback Controlled Electrostatic Energy Analyzer for Use With an Ion Beam Probe Diagnostic System", IEEE Trans. Plasma Sci. 3, pp194-200, December 1975.

8. Stallings, C. H.: J. Appl. Phys. 42, p2831, 1971.

9. Black, W. M. and Robinson, J. W.: J. Appl. Phys. 45, pp2497-2501, June 1974.

10. Ham, Mooyoung and Robinson, J. W.: J. Appl. Phys. 51, pp959-964, February 1980.

11. Javidi, B.: "Secondary Electron Emission from a Charged Dielectric In The Presence of Normal and Oblique Electric Fields", MS Thesis, The Pennsylvania State University, Technical Report, NASA Grant NSG-3166, February 1982.

12. Tilley, D. G.: "Dipole and Quadrupole Synthesis of Electric Potential Fields", MS Thesis, The Pennsylvania State University, NASA CR-1588550, July 1979.

13. Ross, D. P.: "Ion Tracking in an Electrostatic Potential Distribution," NASA-CR-156983, May 1978.

14. Robinson, J. W.: "Mapping of Electrical Potential Distribution With Charged Particle Beams," NASA-CR-158713, June 1979.

15. Quoc-Nguyen, Nguyen: "Secondary Electron Emission from a Dielectric Film Subjected to an Electric Field", MS Thesis, The Pennsylvania State University, NASA-CR-155231, November 1977.

16. Ahlberg, J. H.; Nilson, E. N.; and Walsh, J. L.: Theory of Splines and Their Applications, Academic Press, 1967.

17. Robinson, J. W. and Budd, P. A.: "Oblique-Incidence Secondary Emission From Charged Dielectrics," Spacecraft Charging Technology-1980, NASA Conf. Pub. 2181, pp198-210, November 1980.

18. Budd, P. A.: "Secondary Electron Emission from Electrically Charged Fluorinated-Ethylene-Propylene for Normal and Non-Normal Electron Incidence," MS Thesis, The Pennsylvania State University, NASA-CR-163968, March 1981.

19. Robinson, J. W.: "Mapping of Electrical Potential Distribution With Charged Particle Beams," Semiannual Report, NASA Grant NSG-3166, September 1980.

20. Javidi, B.: Private Communication, 1981.

21. Katz, I. et al: "Extension, Validation, and Application of The NASCAP Code", NASA-CR-159595, January 1979.